Spin-Selective Currents of Tamm Polaritons

Evgeny Sedov,[1,2,3,4,*] Mikhail Glazov,[5] and Alexey Kavokin[1,2,4,6]

[1] *Key Laboratory for Quantum Materials of Zhejiang Province, School of Science, Westlake University, 18 Shilongshan Road, Hangzhou, Zhejiang Province 310024, China*

[2] *Institute of Natural Sciences, Westlake Institute for Advanced Study, 18 Shilongshan Road, Hangzhou, Zhejiang Province 310024, China*

[3] *Vladimir State University Named After A. G. and N. G. Stoletovs, 87 Gorky Str., Vladimir 600000, Russia*

[4] *Spin Optics Laboratory, St-Petersburg State University, 1 Ulyanovskaya, St. Petersburg 198504, Russia*

[5] *Ioffe Institute, 26 Polytechnicheskaya, St. Petersburg 194021, Russia*

[6] *School of Physics and Astronomy, University of Southampton, Highfield, Southampton SO17 1BJ, United Kingdom*

(Received 4 October 2021; revised 20 January 2022; accepted 24 January 2022; published 14 February 2022)

We propose an approach for the excitation of polariton Tamm states with a controllable nontrivial topology. The Tamm polaritons emerge at the interface of two binary one-dimensional photonic crystals belonging to a C_{3v} point group, with an exciton resonance within their matching band gaps. The external magnetic field applied in the Faraday geometry endows the dispersion of the Tamm polaritons with the nonreciprocity: it lifts the degeneracy between opposite propagation directions in the interface plane. The phenomenology of Tamm polariton currents closely resembles one of a Z_2 topological insulator. The proposed structure acts as an optical spin splitter controlled by the magnetic field magnitude.

DOI: 10.1103/PhysRevApplied.17.024037

I. INTRODUCTION

Engineering of energy bands for light in semiconductor heterostructures forms the basis of topological photonics [1,2]. Combining optical structures with different energy band structures one can trigger formation of nontrivial topological objects, namely, surface modes, appearing due to the bulk-edge correspondence [3,4]. In photonics, among such objects are, e.g., surface plasmons emerging at the boundary of a metal and a dielectric [5], optical Tamm states at the interface of two stratified dielectric media [6], and Tamm plasmons at the boundary between a metal and a dielectric Bragg mirror [7,8]. Optical Tamm states are in the focus of our consideration in this paper. They emerge at the interface between two layered photonic structures with overlapping band gaps [6,9]. Such states are topologically protected, in a sense that they are stable against variation of the thicknesses of the layers of the structure in which they arise [10].

The strong light-matter coupling regime and the use of active media that willingly respond to the external impact, electric and magnetic fields, allow one to effectively control optical properties of the whole multilayer system. One of the approaches to achieve the strong coupling regime is embedding quantum wells in all layers of the same refractive index in the structure [11–13]. An alternative approach consists in using bulk materials characterized with an exciton resonance whose energy matches the energy of an optical mode under study [14]. Exciton-polariton modes (polariton modes for brevity) emerge in such structures in the strong light-matter coupling regime [15].

The peculiar property of stratified media is the splitting of the transverse electric (TE or s) and transverse magnetic (TM or p) modes [16,17]. A monotonic increase of its magnitude with the squared in-plane wave vector k^2 for photons is replaced with a more complex dependence for polaritons. The splitting is azimuthally anisotropic and varies with the double azimuth angle. Herewith it does not break the spatial inversion symmetry and keeps the dispersion of the eigenmodes of the structure reciprocal, $\omega(\mathbf{k}) = \omega(-\mathbf{k})$. To introduce spectral nonreciprocity for polariton modes, one can act upon its exciton fraction. It can be done in a controllable way by applying the external fields to the structure.

The nonreciprocal dispersion was demonstrated for optical Tamm states at the interface of two different magnetophotonic crystals [9]. The magnetic field applied in the Voigt geometry breaks the time-reversal symmetry of the system, affecting the TM mode and keeping the TE mode unaffected, so the orthogonal linear polarizations remain independent of each other. In the optical microcavity, the

*evgeny_sedov@mail.ru

spectral symmetry breaking under a combined effect of perpendicular magnetic and electric fields was reported in Ref. [18].

In this work, we demonstrate the possibility of excitation of Tamm polariton states with the spectral nonreciprocity, $\omega(\mathbf{k}) \neq \omega(-\mathbf{k})$, in the presence of an external magnetic field applied in the Faraday geometry. We show that the Tamm resonance in a planar multilayer structure may act as an optical spin splitter triggered by the magnetic field.

II. DETAILS OF THE STRUCTURE

The structure under consideration is schematically shown in Fig. 1. It is formed of two (top and bottom) binary stratified media composed of 14 and 7 pairs of layers SiO_2/CdTe. The bottom structure is grown on the SiO_2 substrate along the $z \parallel [111]$. The choice of the materials is justified as follows. First, the layers of CdTe are active media with the exciton resonance at $\omega_X \approx 1.67$ eV. Second, the high refractive index contrast of the materials estimated as $(n_{b0} - n_a)/n_{b0} \approx 0.46$ results in a strong splitting in the TE and TM polarizations. Third, optical properties of CdTe can be effectively controlled via manipulation of its dielectric tensor $\hat{\varepsilon}_b$ by the external magnetic field [19]. The bulk CdTe is a cubic semiconductor with T_d point symmetry group. The considered structure with the growth axis z oriented along the [111] crystal axis belongs to the C_{3v} point group that is a prerequisite for the discussed effects. The symmetry of the system allows for the magnetospatial dispersion resulting in the bilinear kB terms in the dielectric permittivity, with $\mathbf{k}$ being the light wave vector and $\mathbf{B}$ being the magnetic field. Accordingly, the dielectric tensor can be expanded as $\hat{\varepsilon}_b = \hat{\varepsilon}_b^{(0,0)} + \hat{\varepsilon}_b^{(0,1)}(\mathbf{B}) + \hat{\varepsilon}_b^{(1,1)}(\mathbf{k},\mathbf{B})$. In the considered geometry, the components of this tensor are found to be [19,20]

$$\varepsilon_{b,\alpha\alpha}^{(0,0)} = \varepsilon_{b0}[1 + \omega_{\mathrm{LT}}(\omega_X - \omega - i\Gamma)^{-1}], \tag{1a}$$

$$\varepsilon_{b,xy}^{(0,1)} = -\varepsilon_{b,yx}^{(0,1)} = i\gamma_1 B_z, \tag{1b}$$

$$\frac{\varepsilon_{b,xx}^{(1,1)}}{g} = -\frac{\varepsilon_{b,yy}^{(1,1)}}{g} = \frac{\varepsilon_{b,yz}^{(1,1)}}{h} = \frac{\varepsilon_{b,zy}^{(1,1)}}{h} = -k_x B_z, \tag{1c}$$

$$\frac{\varepsilon_{b,xy}^{(1,1)}}{g} = \frac{\varepsilon_{b,xz}^{(1,1)}}{h} = \frac{\varepsilon_{b,yx}^{(1,1)}}{g} = \frac{\varepsilon_{b,zx}^{(1,1)}}{h} = k_y B_z. \tag{1d}$$

The components not indicated in Eqs. (1) are equal to zero. In Eq. (1a) $\alpha = x,y,z$; ε_{b0} is the background dielectric constant, ω_{LT} is the exciton longitudinal-transverse (LT) splitting frequency, Γ is the nonradiative decay rate. Here γ_1 characterizes the Zeeman splitting, g and h are responsible for the magnetospatial dispersion, and k^2 terms in the bulk exciton dispersion are disregarded. Detailed information on the optical properties of CdTe can be found in Appendix A.

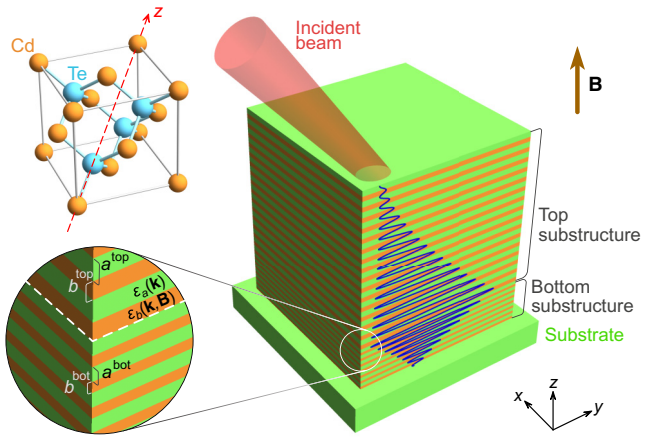

FIG. 1. Schematic of the excitation of the Tamm polariton. The external magnetic field **B** is applied in the structure growth direction. The inset shows the unit cell of CdTe in the coordinate system considered in the manuscript with $z \parallel [111]$.

The bottom substructure is the Bragg mirror with the polariton resonance at the edge of its first photonic band gap. In the top substructure the Bragg condition is violated so that the second photonic band gap opens. Because of almost twice wider layers of the top substructure, its second band gap overlaps with the first band gap of the bottom substructure.

III. CHARACTERIZATION OF TAMM POLARITON STATES

The condition for the emergence of the Tamm polariton states can be obtained following the approach developed for calculation of Tamm plasmons in Ref. [7]. Let us consider two oppositely directed waves propagating from the interface to the top substructure and to the bottom substructure. Reflection of the corresponding waves is characterized by the amplitude reflection coefficient matrix of the form $\hat{r}_{ij}^L$, where $L = \mathrm{top}, \mathrm{bottom}$, and $i,j = s,p$ indicate the polarization of the incident (first index) and reflected (second index) wave at the interface. The diagonal terms, r_{pp}^L and r_{ss}^L, characterize reflection of the wave without the change of its polarization. The magnetic field mixes the polarizations of the waves, so the off-diagonal terms, r_{ps}^L and r_{sp}^L, characterize the rotation of the polarization upon reflection. In order to enable the existence of the Tamm state, the field of a given polarization entering the top (bottom) substructure should match the field of the same polarization reflected from the bottom (top) substructure. The condition for the Tamm polariton state formation takes the form

$$(r_{ii}^{\mathrm{top}} r_{ii}^{\mathrm{bot}} + r_{ji}^{\mathrm{top}} r_{ij}^{\mathrm{bot}}) f_p + (r_{jj}^{\mathrm{top}} r_{jj}^{\mathrm{bot}} + r_{ij}^{\mathrm{top}} r_{ji}^{\mathrm{bot}}) f_s = f_i, \tag{2}$$

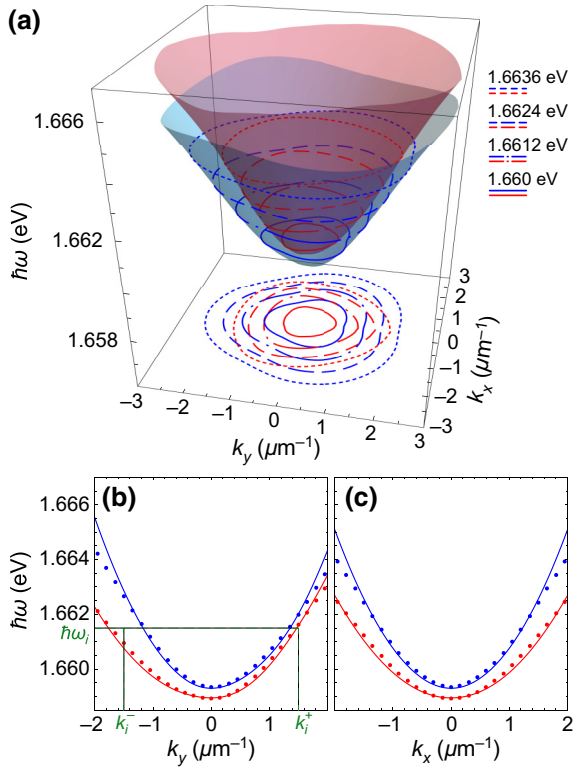

FIG. 2. (a) Dispersion of orthogonally polarized Tamm polariton states at $B_z = 10$ T calculated using TMM. Contours of the same line type correspond to the same energy. (b),(c) Dispersions of Tamm states obtained from TMM (dots) and from Hamiltonian (3) (solid lines) at $k_x = 0$ (b) and $k_y = 0$ (c). Dashed lines in (b) indicate the parameters used for Fig. 3.

where $i,j = s,p$ and $f_s = \sin\theta, f_p = \cos\theta$, with the complex parameter θ that characterizes both the angle of the polarization plane and ellipticity of polarization. See Appendices B–D for details of the derivation of Eq. (2). In the absence of the magnetic field ($\mathbf{B} = 0$) the TE and TM polarizations are decoupled and condition (2) reduces to $r_{ii}^{\text{top}} r_{ii}^{\text{bot}} = 1$, and $r_{ij}^{L} = 0$.

The dispersion of the doublet of the polariton Tamm states in the cavity plane calculated using the generalized 4×4 transfer matrix method (TMM) [21–24] in the presence of the external magnetic field ($B_z = 10$ T) is shown in Fig. 2(a). Details of TMM are presented in Appendices B–C. Values of the parameters used in this calculation are given in Ref. [25]. The orientation of the dispersion surface is defined by the choice of coordinate axes. We use here the frame with $x \parallel [11\bar{2}]$, $y \parallel [\bar{1}10]$, and $z \parallel [111]$ being the growth axis of the structure (see the inset in Fig. 1). Note that, for this choice of axes, the threefold rotation axis $C_3 \parallel z$, and one of three vertical reflection planes is (xz), i.e., the reflection $y \to -y$ is present in the symmetry group of the structure resulting from the magnetic response of the CdTe layers.

The effective 2×2 Hamiltonian for the polariton doublet of the Tamm states can be derived by the method of invariants and takes the form

$$H = \frac{\hbar^2 k^2}{2m^*} + C_1 S_z B_z + C_2[(k_x^2 - k_y^2)S_x + 2k_x k_y S_y] + C_3(k_x S_y + k_y S_x)B_z. \quad (3)$$

The Hamiltonian acts on the spinor $E = [E_+(\mathbf{r}), E_-(\mathbf{r})]^{\mathrm{T}}$ characterizing electric field in the right-circularly, $E_+(\mathbf{r})$, and left-circularly, $E_-(\mathbf{r})$, polarized components. Here we introduced the pseudospin operator $\hat{\mathbf{S}} = (S_x, S_y, S_z)$, with S_α ($\alpha = x,y,z$) being the 2×2 Pauli matrices, the unit matrix in Eq. (3) is omitted, and $\mathbf{k} = (k_x, k_y)$ is the polariton in-plane wave vector. The Hamiltonian is parametrized by four constants: m^* being the effective mass and $C_1, \ldots, C_3$ are responsible for the effective magnetic fields acting on the polariton pseudospin. The S_z component of the pseudospin is responsible for the circular polarization. It transforms as the z component of the magnetic field $\mathbf{B}$. The constant C_1 is responsible for the Zeeman splitting; the constant C_2 describes the exciton longitudinal-transverse splitting. The term with C_3 arises in the C_{3v} point symmetry only; it is responsible for the magnetospatial dispersion—see Ref. [26]. In Eq. (3) we take into account the terms up to k^2. See Appendix E for details of derivations of the nonmagnetic part of the Hamiltonian.

Effective Hamiltonian (3) can be readily diagonalized as

$$\mathcal{E}_\pm(\mathbf{k}) = \frac{\hbar^2 k^2}{2m^*} \pm \delta_{\mathbf{k}}, \quad (4)$$

where

$$\delta_{\mathbf{k}} = \sqrt{B_z^2(C_3^2 k^2 + C_1^2) + C_2^2 k^4 + 2C_2 C_3 B_z k^3 \sin 3\varphi} \quad (5)$$

and φ is the angle between the wave vector and x axis. Eigenenergies (4) are illustrated in Figs. 2(b) and 2(c) in comparison with the results of TMM calculations. A good agreement between the TMM and effective Hamiltonian approach is seen; see Ref. [27] for the parameters of Eq. (3). One can readily check that the spectrum at $\mathbf{B} \neq 0$ always has a gap at small k. Indeed, the Hamiltonian can be presented as

$$H = \hbar^2 k^2 / 2m^* + (\boldsymbol{\delta}_{\mathbf{k}} \mathbf{S}), \quad (6)$$

where $\boldsymbol{\delta}_{\mathbf{k}}$ is a vector governed by B_z and $\mathbf{k}$, whose absolute value is given by Eq. (5). To close the gap, $\delta_{\mathbf{k}}$ should turn to zero, which is possible only at $B_z = 0$. In fact, the magnetic field opens a gap in the spectrum of two-dimensional Tamm polaritons.

Depending on the parameters, the gap can have a topological nature and, as a result, the system will demonstrate

nontrivial one-dimensional edge states. To demonstrate the effect, we derive the Berry curvature

$$\mathcal{F}_{xy}^{\pm} = \mp \frac{1}{2\delta_{\mathbf{k}}^3} \boldsymbol{\delta}_{\mathbf{k}} \cdot (\partial_{k_x} \boldsymbol{\delta}_{\mathbf{k}} \times \partial_{k_y} \boldsymbol{\delta}_{\mathbf{k}}), \tag{7}$$

where the $\pm$ signs refer to the upper and lower bands in Eq. (4), respectively, and calculate the Chern numbers as

$$\mathcal{C}^{\pm} = 2\pi \sum_{\mathbf{k}} \mathcal{F}_{xy}^{\pm} = \mp \int_0^{\infty} dk k \int_0^{2\pi} \frac{d\varphi}{2\pi} C_1 B_z \frac{C_2 k^2 - (C_3 B_z/2)^2}{4\delta^2}, \tag{8}$$

with the result

$$\mathcal{C}^{\pm} = \mp \operatorname{sign} C_1 B_z \quad \text{at } C_2 \neq 0. \tag{9}$$

Note that at $C_2 = 0$ the Hamiltonian's topological properties are ill-defined, and Eq. (8) gives half-integer Chern numbers [28]. Interestingly, the Chern numbers do not depend on $C_3 \neq 0$ as can be verified by decomposing the subintegral expression in the series in C_3. Hamiltonian (3) at small k is analogous to the Hamiltonian describing electronic states in the two-dimensional Z_2 topological insulator.

IV. MAGNETICALLY CONTROLLED TAMM POLARITONS

The nonreciprocity of the spectrum of the Tamm polariton doublet results in its featured intensity and polarization properties. In Fig. 3 we show the distribution of the intensity, $I = E^{\dagger}E$, and the polarization components, $s_{\alpha} = (E^{\dagger} S_{\alpha} E)/I$ $(\alpha = x, y, z)$, in the plane (y, z) of the polariton states excited by the incident beam of a Gaussian shape $E_i \propto \exp[-y^2/2w^2] \exp[i(k_i^{\pm} y - \omega_i t)]$ of width $w = 3$ μm. The energy $\hbar\omega_i$ and the wave number $k_i^{\pm}$ are taken to be 1.6615 eV and ± 1.5 μm^{-1}, respectively. The polarization of the incident beam is taken to be right circular, $(1, 0)^{\mathrm{T}}$. The distribution of the spatial spectrum in the structure growth direction is shown in Fig. 4. As one can see in Fig. 2(b), in the case of $k_y = k_i^{+} > 0$ (right panels in Fig. 3) the TE-TM splitting vanishes and the incident beam is close to the resonance with both components of the Tamm polariton doublet. The spectra of the two branches merge and form a single maximum close to the incident wave vector in Fig. 3(e). The incident energy is effectively transferred to the Tamm state localized at the interface of the two substructures. The reflected beam is weakly pronounced, and it is mostly manifested in the formation of the interference fringes in the upper part of Figs. 3(e) and 4(e). The Tamm polariton inherits the circular polarization of the incident beam; see Figs. 3(h) and 4(h).

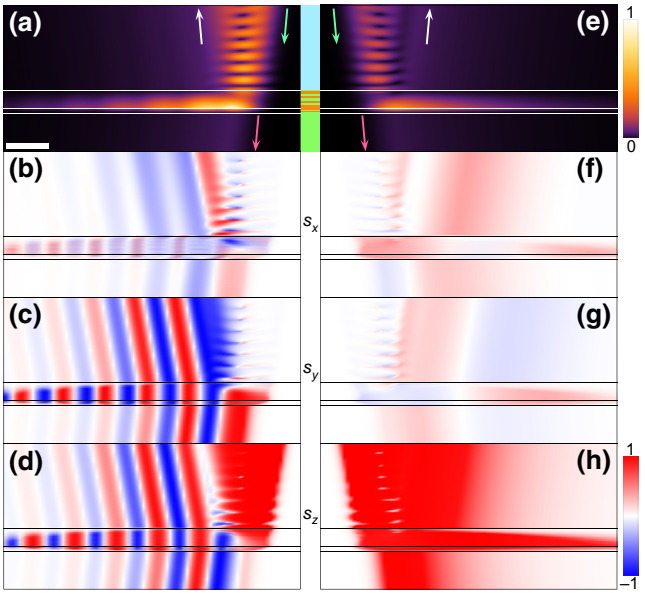

FIG. 3. Polariton Tamm states excited by inclined Gaussian beams with $\hbar\omega_i = 1.6615$ eV, $k_y = k_i^{-} = -1.5$ μm^{-1} (a)–(d) and $k_y = k_i^{+} = 1.5$ μm^{-1} (e)–(h). The width of the beams is $w = 3$ μm. The polarization of the excitation beam is right circular. Green, pink, and white arrows in (a) and (e) indicate directions of the incident, transmitted, and reflected beams, respectively. The inset between (a) and (e) shows schematically the considered structure. Horizontal lines in each panel indicate (from top to bottom) the "air-top substructure," "top substructure-bottom substructure," and "bottom substructure-substrate" interfaces. The white bar in (a) corresponds to 10 μm.

The Tamm polariton mode propagating in the opposite direction ($k_y = k_i^{-} < 0$) considerably differs from the state discussed above (left panels in Figs. 3 and 4). The center of the spectrum of the incident beam, k_i^{-}, is far from resonance with both eigenmodes. It is separated from them by more than 0.25 μm^{-1}. This results in a much more pronounced reflected beam. Because of the strong TE-TM splitting at the incident energy $\hbar\omega_i$, the propagation constants of the orthogonally polarized components of the Tamm polariton state along the interface differ from each other by more than 0.5 μm^{-1}. One can see two clearly distinguishable maxima in Fig. 4(a) distant from k_i^{-}. The intensity and the polarization distribution of the emerging Tamm polariton state experience beats in real space. Figure 3(a) shows the intensity distribution of the Tamm state that is periodically modulated along the propagation direction y. The pure circular polarization of the incident beam, Fig. 3(d), converts to the polarization patterns representing alternating domains of diagonal and circular polarizations of the Tamm polariton state; cf. Figs. 3(g), 3(h) and Figs. 3(c), 3(d). In the reciprocal space, the two lines possess orthogonal linear polarizations; see Fig. 4(b). The period of oscillations of both intensity and polarization distributions is determined by the magnitude of the

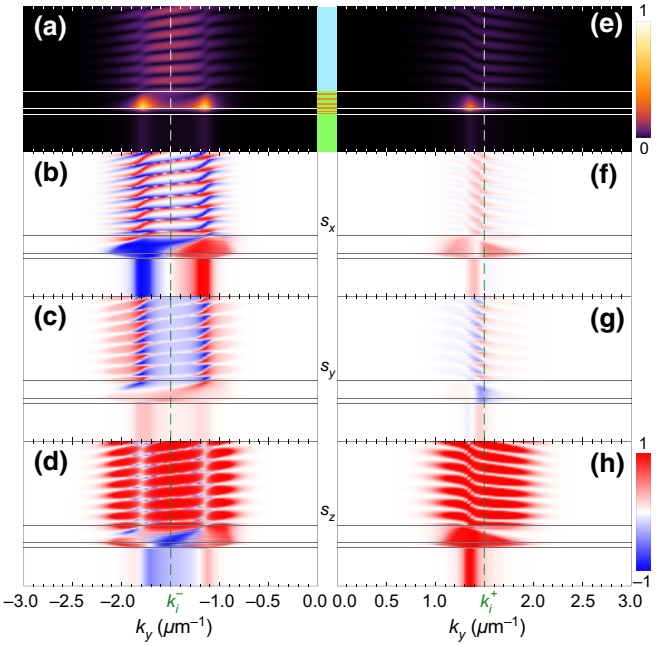

FIG. 4. Distribution in the (k_y, z) plane of the polariton Tamm states shown in Fig. 3. The dashed line indicates the incident beam wave vector $k_y = k_i^- = -1.5\ \mu\text{m}^{-1}$ (a)–(d) and $k_y = k_i^+ = 1.5\ \mu\text{m}^{-1}$ (e)–(h). The parameters used for calculations are the same as for Fig. 3.

TE-TM splitting and is about 10 μm^{-1}. The formation of alternating polarization patterns due the interference of energy split eigenmodes is the manifestation of the optical spin Hall effect: the phenomenon is well known for polaritons in optical microcavities [29–31]. The form of Hamiltonian (3) indicates the possibility of manifestation in the proposed structure of another polarization-splitting-induced effect known in microcavities, that is, the zitterbewegung [32–34]. The effect is expected to manifest itself as oscillations of the trajectory of the Tamm polariton in the interface plane accompanying the oscillations of the polarization.

V. CONCLUSION

We have proposed a resonant optical structure that supports formation of Tamm polariton states with the controllable nonreciprocal dispersion. The Tamm states emerge at the interface of two substructures representing stratified media belonging to the C_{3v} symmetry group with merging odd and even band gaps. The nonreciprocity of the spectrum emerges under the external magnetic field applied in the Faraday geometry. The magnetospatial dispersion endows the polarization properties of the structure with the nonreciprocity and gives a wide control over the polarization of the Tamm polariton states. We would like to underline that a homogeneous planar multilayer structure discussed here is easy to fabricate, in contrast to two-dimensional patterned structures used for realization of polariton topological insulators in the previous works [35]. The simplicity of design makes structures that sustain Tamm modes especially attractive for applications in topological polaritonics.

ACKNOWLEDGMENTS

A.K. acknowledges the support of Westlake University, Project 041020100118 and Program 2018R01002 funded by Leading Innovative and Entrepreneur Team Introduction Program of Zhejiang Province of China. The Russian Foundation for Basic Research (Grant No. 21-52-10005), Saint-Petersburg State University (Grant No. 91182694), the Grant of the President of the Russian Federation for state support of young Russian scientists (No. MK-4729.2021.1.2), and the Royal Society International Exchange Grant No. IEC/R2/202148 are acknowledged.

APPENDIX A: CHARACTERIZATION OF THE MATERIALS FORMING THE STRUCTURE

The structure considered in the manuscript is composed of two SiO_2/CdTe substructures. The SiO_2 layers are considered optically isotropic, characterized by the dielectric constant $\varepsilon_a = 2.25$. Bulk CdTe is a cubic semiconductor with T_d point symmetry group. The dielectric tensor of CdTe can be represented as [19,36,37]

$$\hat{\varepsilon}_b = \hat{\varepsilon}_b^{(0,0)} + \hat{\varepsilon}_b^{(0,1)}(\mathbf{B}) + \hat{\varepsilon}_b^{(1,1)}(\mathbf{k}, \mathbf{B}). \tag{A1}$$

The first term on the right-hand side of Eq. (A1), $\hat{\varepsilon}_b^{(0,0)}$, corresponds to no magnetic field and spatial dispersion. Its components coincide with Eq. (1a) in the rotated frame. The components of the linear in $\mathbf{B}$ term, $\hat{\varepsilon}_b^{(0,1)}(\mathbf{B})$, are given as

$$\varepsilon_{b,\alpha\beta}^{(0,1)} = i\gamma_1 \delta_{\alpha\beta\zeta} B_\zeta, \quad \alpha, \beta, \zeta = x, y, z. \tag{A2}$$

Here γ_1 is responsible for the Faraday effect and $\delta_{\alpha\beta\zeta}$ is the Levi-Civita symbol. The components of the bilinear term, $\hat{\varepsilon}_b^{(1,1)}(\mathbf{k}, \mathbf{B})$, in Eq. (A1) are given by

$$\varepsilon_{b,\alpha\alpha}^{(1,1)} = \gamma_2 (k_{\alpha+1} B_{\alpha+1} - k_{\alpha+2} B_{\alpha+2}), \tag{A3a}$$

$$\varepsilon_{b,\alpha\beta}^{(1,1)} = \gamma_3 [\mathbf{B} \times \mathbf{k}]_\zeta. \tag{A3b}$$

The constants γ_2 and γ_3 above describe the magnetospatial dispersion. The cyclic rule is applied in Eq. (A3): $\alpha + 3 = \alpha\ (1, 2, 3 \to x, y, z)$.

In Eqs. (A1)–(A3) the axes x, y, and z are oriented along the crystal axes [100], [010], and [001], respectively. The structure joins the C_{3v} point group when the z axis is oriented in the [111] direction. To bring the dielectric tensor $\hat{\varepsilon}_b$ to the new coordinates, we perform the

transformation

$$\hat{\varepsilon}_b \to \hat{R}\hat{\varepsilon}_b\hat{R}^{-1}, \tag{A4}$$

where $\hat{R} = \hat{R}_Z(a_1)\hat{R}_X(a_2)\hat{R}_Z(a_3)$ is the rotation matrix composed of elemental rotation matrices

$$\hat{R}_Z(a_{1,3}) = \begin{pmatrix} \cos a_{1,3} & -\sin a_{1,3} & 0 \\ \sin a_{1,3} & \cos a_{1,3} & 0 \\ 0 & 0 & 1 \end{pmatrix}, \tag{A5a}$$

$$\hat{R}_X(a_2) = \begin{pmatrix} 1 & 0 & 0 \\ 0 & \cos a_2 & -\sin a_2 \\ 0 & \sin a_2 & \cos a_2 \end{pmatrix}. \tag{A5b}$$

For rotating z from [001] to [111], one should take the following Euler angles: $a_1 = 0$, $a_2 \approx 54.736^\circ$, and $a_3 = 45^\circ$. The vectors transform with respect to $\mathbf{k} \to \hat{R}^{-1}\mathbf{k}$ and $\mathbf{B} \to \hat{R}^{-1}\mathbf{B}$. We keep only the component B_z of the magnetic field in the new coordinates. With that said, in the new axes the components of the dielectric tensor $\hat{\varepsilon}_b$ take the form (1) with $g = (\gamma_2 - 2\gamma_3)/\sqrt{6}$ and $h = (\gamma_2 + \gamma_3)/\sqrt{3}$.

APPENDIX B: MAXWELL'S EQUATIONS

Without loss of generality, we consider the propagation in the x-z plane, assuming that $k_y = 0$ in Eq. (1). Another propagation plane can be chosen by rotating the tensor $\hat{\varepsilon}_b$ around the z axis. According to the continuity conditions at the interfaces, we get the following expressions for the components of the wave vector in layer j:

$$k_{xj} = k_{x0} = k_0 q, \quad k_{yj} = k_{y0} = 0, \quad k_{zj} = k_0\kappa_j. \tag{B1}$$

Here $\mathbf{k}_0$ is the wave vector of the incident wave, $k_0 = \omega_0/c$, ω_0 is the angular frequency of the wave. For convenience, we have introduced the dimensionless quantities q and κ_j for the in-plane and out-of-plane wave vector components, respectively. Maxwell's equations in layer j can be written in matrix form as [24]

$$\begin{pmatrix} \varepsilon_{xx} - \kappa_j^2 & \varepsilon_{xy} & \varepsilon_{xz} + q\kappa_j \\ \varepsilon_{yx} & \varepsilon_{yy} - q^2 - \kappa_j^2 & \varepsilon_{yz} \\ \varepsilon_{zx} + q\kappa_j & \varepsilon_{zy} & \varepsilon_{zz} - q^2 \end{pmatrix} \begin{pmatrix} E_x \\ E_y \\ E_z \end{pmatrix} = 0. \tag{B2}$$

The in-plane wave vector component q is conserved when crossing the interfaces of the layers, and it is determined by inclination of the incident beam. The out-of-plane propagation constant κ_j is different in different layers, and it can be found from the equation

$$\begin{vmatrix} \varepsilon_{xx} - \kappa_j^2 & \varepsilon_{xy} & \varepsilon_{xz} + q\kappa_j \\ \varepsilon_{yx} & \varepsilon_{yy} - q^2 - \kappa_j^2 & \varepsilon_{yz} \\ \varepsilon_{zx} + q\kappa_j & \varepsilon_{zy} & \varepsilon_{zz} - q^2 \end{vmatrix} = 0, \tag{B3}$$

which has four roots in the general case. These roots numbered as κ_{jl} ($l = 1, 2, 3, 4$) characterize four eigenmodes of the electric field. They represent waves of two orthogonal polarizations (s and p) propagating in the forward ($\to$) and backward ($\leftarrow$) directions. The electric field is then represented in the form of a four-component vector:

$$\mathbf{E} = \begin{pmatrix} E^p_{\to} \\ E^s_{\to} \\ E^p_{\leftarrow} \\ E^s_{\leftarrow} \end{pmatrix} = \begin{pmatrix} E_1 \\ E_2 \\ E_3 \\ E_4 \end{pmatrix}. \tag{B4}$$

APPENDIX C: 4 × 4 TRANSFER MATRIX

To examine propagation of light through an anisotropic stratified medium, we use the generalized 4×4 transfer matrix formalism [21,22] capable of treating optical degeneracies arising in isotropic embedded layers [23,24]. The electric fields in layers j and $j-1$ are interlinked as

$$\mathbf{E}_{j-1} = \hat{A}_{j-1}^{-1}\hat{A}_j\hat{P}_j\mathbf{E}_j, \tag{C1}$$

where $\hat{P}_j$ is the 4×4 propagation matrix with the components determined as $P_{j,ll'} = \delta_{ll'}\exp[-ik_0\kappa_{jl}d_j]$. Here $\delta_{ll'}$ is the Kronecker delta and d_j is the thickness of the jth layer. The interaction matrix $\hat{A}_j$ takes the form

$$\hat{A}_j = \begin{pmatrix} a_{j11} & a_{j21} & a_{j31} & a_{j41} \\ a_{j12} & a_{j22} & a_{j32} & a_{j42} \\ b_{j11} & b_{j21} & b_{j31} & b_{j41} \\ b_{j12} & b_{j22} & b_{j32} & b_{j42} \end{pmatrix}, \tag{C2}$$

where the components are given by [23,24]

$$a_{j11} = a_{j22} = a_{j42} = -a_{j31} = 1, \tag{C3a}$$

$$a_{j12} = \begin{cases} 0, & \kappa_{j1} = \kappa_{j2}, \\ \dfrac{\varepsilon^j_{yz}(\varepsilon^j_{zx} + q\kappa_{j1}) - \varepsilon^j_{yx}(\varepsilon^j_{zz} - q^2)}{(\varepsilon^j_{zz} - q^2)(\varepsilon^j_{yy} - q^2 - \kappa^2_{j1}) - \varepsilon^j_{yz}\varepsilon^j_{zy}}, & \kappa_{j1} \neq \kappa_{j2}, \end{cases} \tag{C3b}$$

$$a_{j13} = \begin{cases} -\dfrac{(\varepsilon^j_{zx} + q\kappa_{j1})}{\varepsilon^j_{zz} - q^2}, & \kappa_{j1} = \kappa_{j2}, \\ -\dfrac{(\varepsilon^j_{zx} + q\kappa_{j1})}{\varepsilon^j_{zz} - q^2} - \dfrac{\varepsilon^j_{zy}}{\varepsilon^j_{zz} - q^2}a_{12}, & \kappa_{j1} \neq \kappa_{j2}, \end{cases} \tag{C3c}$$

$$a_{j21} = \begin{cases} 0, & \kappa_{j1} = \kappa_{j2}, \\ \dfrac{\varepsilon^j_{zy}(\varepsilon^j_{xz} + q\kappa_{j2}) - \varepsilon^j_{xy}(\varepsilon^j_{zz} - q^2)}{(\varepsilon^j_{zz} - q^2)(\varepsilon^j_{xx} - \kappa^2_{j2}) - (\varepsilon^j_{xz} + q\kappa_{j2})(\varepsilon^j_{zx} + q\kappa_{j2})}, & \kappa_{j1} \neq \kappa_{j2}, \end{cases} \tag{C3d}$$

$$a_{j23} = \begin{cases} -\dfrac{\varepsilon^j_{zy}}{\varepsilon^j_{zz} - q^2}, & \kappa_{j1} = \kappa_{j2}, \\ -\dfrac{\varepsilon^j_{zx} + q\kappa_{j2}}{\varepsilon^j_{zz} - q^2} a_{21} - \dfrac{\varepsilon^j_{zy}}{\varepsilon^j_{zz} - q^2}, & \kappa_{j1} \neq \kappa_{j2}, \end{cases} \tag{C3e}$$

$$a_{j32} = \begin{cases} 0, & \kappa_{j3} = \kappa_{j4}, \\ \dfrac{\varepsilon^j_{yx}(\varepsilon^j_{zz} - q^2) - \varepsilon^j_{yz}(\varepsilon^j_{zx} + q\kappa_{j3})}{(\varepsilon^j_{zz} - q^2)(\varepsilon^j_{yy} - q^2 - \kappa^2_{j3}) - \varepsilon^j_{yz}\varepsilon^j_{zy}}, & \kappa_{j3} \neq \kappa_{j4}, \end{cases} \tag{C3f}$$

$$a_{j33} = \begin{cases} \dfrac{(\varepsilon^j_{zx} + q\kappa_{j3})}{\varepsilon^j_{zz} - q^2}, & \kappa_{j3} = \kappa_{j4}, \\ \dfrac{(\varepsilon^j_{zx} + q\kappa_{j3})}{\varepsilon^j_{zz} - q^2} + \dfrac{\varepsilon^j_{zy}}{\varepsilon^j_{zz} - q^2} a_{32}, & \kappa_{j3} \neq \kappa_{j4}, \end{cases} \tag{C3g}$$

$$a_{j41} = \begin{cases} 0, & \kappa_{j3} = \kappa_{j4}, \\ \dfrac{\varepsilon^j_{zy}(\varepsilon^j_{xz} + q\kappa_{j4}) - \varepsilon^j_{xy}(\varepsilon^j_{zz} - q^2)}{(\varepsilon^j_{zz} - q^2)(\varepsilon^j_{xx} - \kappa^2_{j4}) - (\varepsilon^j_{xz} + q\kappa_{j4})(\varepsilon^j_{zx} + q\kappa_{j4})}, & \kappa_{j3} \neq \kappa_{j4}, \end{cases} \tag{C3h}$$

$$a_{j43} = \begin{cases} -\dfrac{\varepsilon^j_{zy}}{\varepsilon^j_{zz} - q^2}, & \kappa_{j3} = \kappa_{j4}, \\ -\dfrac{\varepsilon^j_{zx} + q\kappa_{j4}}{\varepsilon^j_{zz} - q^2} a_{j41} - \dfrac{\varepsilon^j_{zy}}{\varepsilon^j_{zz} - q^2}, & \kappa_{j3} \neq \kappa_{j4}, \end{cases} \tag{C3i}$$

$$b_{jl1} = \kappa_{jl} a_{jl1} - q a_{jl3}, \tag{C3j}$$

$$b_{jl2} = \kappa_{jl} a_{jl2}, \quad l = 1, 2, 3, 4. \tag{C3k}$$

Different expressions for $a_{jll'}$ for degenerate and nondegenerate propagation constants allow avoiding singularities in the interface matrix $\hat{A}_j$. The vectors $\mathbf{a}_{jl} = (a_{jl1}, a_{jl2}, a_{jl3})$ have to be normalized as $\mathbf{a}_{jl} = \mathbf{a}_{jl}/|\mathbf{a}_{jl}|$. The following equation links the input field E_0 with the field in the j th layer of the structure:

$$\mathbf{E}_0 = \hat{T}\mathbf{E}_j = \hat{A}_0^{-1}\hat{A}_1\hat{P}_1\hat{A}_1^{-1}\hat{A}_2\hat{P}_2 \cdots \hat{A}_{j-1}^{-1}\hat{A}_j\hat{P}_j\mathbf{E}_j. \tag{C4}$$

APPENDIX D: THE TAMM MODES

For pure p- and s-polarized incident waves, the reflection and transmission coefficients are calculated as

$$r_{pp} = \left(\frac{E^p_{\text{refl}}}{E^p_{\text{inc}}}\right)_{E^s_{\text{inc}}=0} = \frac{T_{31}T_{22} - T_{32}T_{21}}{T_{11}T_{22} - T_{12}T_{21}}, \tag{D1a}$$

$$r_{ss} = \left(\frac{E^s_{\text{refl}}}{E^s_{\text{inc}}}\right)_{E^p_{\text{inc}}=0} = \frac{T_{11}T_{42} - T_{41}T_{12}}{T_{11}T_{22} - T_{12}T_{21}}, \tag{D1b}$$

$$r_{ps} = \left(\frac{E^s_{\text{refl}}}{E^p_{\text{inc}}}\right)_{E^s_{\text{inc}}=0} = \frac{T_{41}T_{22} - T_{42}T_{21}}{T_{11}T_{22} - T_{12}T_{21}}, \tag{D1c}$$

$$r_{sp} = \left(\frac{E^p_{\text{refl}}}{E^s_{\text{inc}}}\right)_{E^p_{\text{inc}}=0} = \frac{T_{11}T_{32} - T_{31}T_{12}}{T_{11}T_{22} - T_{12}T_{21}}, \tag{D1d}$$

$$t_{pp} = \left(\frac{E^p_{\text{trans}}}{E^p_{\text{inc}}}\right)_{E^s_{\text{inc}}=0} = \frac{T_{22}}{T_{11}T_{22} - T_{12}T_{21}}, \tag{D1e}$$

$$t_{ss} = \left(\frac{E^s_{\text{trans}}}{E^s_{\text{inc}}}\right)_{E^p_{\text{inc}}=0} = \frac{T_{11}}{T_{11}T_{22} - T_{12}T_{21}}, \tag{D1f}$$

$$t_{ps} = \left(\frac{E^s_{\text{trans}}}{E^p_{\text{inc}}}\right)_{E^s_{\text{inc}}=0} = \frac{-T_{21}}{T_{11}T_{22} - T_{12}T_{21}}, \tag{D1g}$$

$$t_{sp} = \left(\frac{E^p_{\text{trans}}}{E^s_{\text{inc}}}\right)_{E^p_{\text{inc}}=0} = \frac{-T_{12}}{T_{11}T_{22} - T_{12}T_{21}}, \tag{D1h}$$

where the diagonal terms r_{ss} (t_{ss}) and r_{pp} (t_{pp}) are the reflection (transmission) coefficients for the TE or s and TM or p modes. The off-diagonal components $r_{ps,sp}$ ($t_{ps,sp}$) describe a partial transfer to an opposite mode on reflection (transmission). Here $E^{s,p}_{\text{inc, refl, trans}}$ are the incident, reflected from, and transmitted through the structure field amplitudes of the corresponding polarizations. Following Ref. [38], we should note that in anisotropic structures we have to deal with ordinary (o) and extraordinary (e) modes instead of p and s modes. So, to reflect the physical meaning of the transmission coefficients more pedantically, one should have used the following notation for them: $t_{p(p/o)}$, $t_{s(s/e)}$, $t_{p(s/e)}$, $t_{s(p/o)}$ with p and s in parentheses for isotropic media and o and e for anisotropic media [39].

Let us now virtually split the structure into two substructures along the interface of the two Bragg mirrors. The field propagating *from the interface to the bottom mirror* is described as

$$\mathbf{E}^{\text{bot}}_{\text{inc}} = \begin{pmatrix} E^p_{\rightarrow} \\ E^s_{\rightarrow} \\ E^p_{\leftarrow} \\ E^s_{\leftarrow} \end{pmatrix} = \begin{pmatrix} E^p_{\rightarrow} \\ E^s_{\rightarrow} \\ r^{\text{bot}}_{pp}E^p_{\rightarrow} + r^{\text{bot}}_{sp}E^s_{\rightarrow} \\ r^{\text{bot}}_{ss}E^s_{\rightarrow} + r^{\text{bot}}_{ps}E^p_{\rightarrow} \end{pmatrix}. \tag{D2}$$

In the transmitted field on the right-hand side of Eq. (D2) we have only transmitted components and no reflected components. The same procedure for the field propagating *from the interface to the top mirror* written in the same basis gives

$$\mathbf{E}^{\text{top}}_{\text{inc}} = \begin{pmatrix} E^p_{\rightarrow} \\ E^s_{\rightarrow} \\ E^p_{\leftarrow} \\ E^s_{\leftarrow} \end{pmatrix} = \begin{pmatrix} r^{\text{top}}_{pp}E^p_{\leftarrow} + r^{\text{top}}_{sp}E^s_{\leftarrow} \\ r^{\text{top}}_{ss}E^s_{\leftarrow} + r^{\text{top}}_{ps}E^p_{\leftarrow} \\ E^p_{\leftarrow} \\ E^s_{\leftarrow} \end{pmatrix}. \tag{D3}$$

We take the field going from top to bottom as $(E^p_{\rightarrow}, E^s_{\rightarrow}) = (\cos\theta, \sin\theta)$, i.e., we parametrize it with the complex parameter θ that defines polarization (both angle and ellipticity) of the field. For the Tamm state to exist, the field of a given polarization entering the top mirror should match the field of the same polarization reflected from the bottom mirror. And vice versa, the field reflected from the top mirror should match the field entering the bottom mirror. Eliminating the components $E^p_{\leftarrow}$ and $E^s_{\leftarrow}$ from Eqs. (D2) and (D3), we arrive at the equation for the Tamm state, Eq. (2), with the variables (ω, θ).

APPENDIX E: THE DERIVATION OF THE EFFECTIVE HAMILTONIAN OF THE TAMM STATE

Let us consider an optically active exciton in a cubic semiconductor crystal. The three optically active states have a total angular momentum $L = 1$ (the polarization induced by the exciton **P** is a vector); therefore, it is convenient to express the effective Hamiltonian in terms of the basis matrices of the angular momentum 1: L_x, L_y, L_z, and their combinations. According to the general theory of angular momentum, the set of three matrices **L** can be treated as a pseudovector. In the isotropic approximation, the effective Hamiltonian accounting terms with powers of the wave vector **k** up to two, has the form

$$\mathcal{A}k^2 + \mathcal{B}(\mathbf{L}\cdot\mathbf{k})^2, \tag{E1}$$

where $\mathcal{A}$ and $\mathcal{B}$ are parameters. We omit the identity matrix for brevity. It is seen that the energy of the "longitudinal" exciton $E_L = \mathcal{A}k^2$ differs from the energy of the two "transverse" states, $E_T = (\mathcal{A}+\mathcal{B})k^2$, which is easy to see directing **k** along the z axis. We should note that in reality the spectrum of longitudinal and transverse excitons differs from these simplest formulae; one should take into account the polariton effects. Herewith, the degeneracy multiplicities are preserved, and the polarization of states is described correctly.

Let us now turn to a two-dimensional (or quasi-two-dimensional) model, assuming that $\mathbf{k} \parallel (xy)$, and dimensional quantization and deformation split off a state polarized along the z axis by a significant energy. In the axial approximation, the effective Hamiltonian is written as

$$H_{\text{ax}} = \mathcal{A}k^2 + \mathcal{B}(\mathbf{L}\cdot\mathbf{k})^2 + \mathcal{C}L_z^2, \tag{E2}$$

where the term with $\mathcal{C}L_z^2$ is the splitting of the triplet into the z state and the doublet polarized in the (xy) plane.

Assuming that $\mathcal{B}k^2 \ll \mathcal{C}$ we can consider the doublet independently from the z state. We note that

$$(\mathbf{L}\cdot\mathbf{k})^2 = L_x^2k^2 + L_y^2k_y^2 + (L_xL_y + L_yL_x)k_xk_y, \tag{E3}$$

and use the explicit matrix form of **L**:

$$L_x^2 = \frac{1}{2}\begin{pmatrix} 1 & 0 & 1 \\ 0 & 2 & 0 \\ 1 & 0 & 1 \end{pmatrix}, \tag{E4a}$$

$$L_y^2 = \frac{1}{2}\begin{pmatrix} 1 & 0 & -1 \\ 0 & 2 & 0 \\ -1 & 0 & 1 \end{pmatrix}, \tag{E4b}$$

$$L_xL_y + L_yL_x = \begin{pmatrix} 0 & 0 & -\mathrm{i} \\ 0 & 0 & 0 \\ \mathrm{i} & 0 & 0 \end{pmatrix}. \tag{E4c}$$

We introduce the pseudospin vector $\mathbf{S} = (S_x, S_y, S_z)$, where $S_{x,y,z}$ are the Pauli matrices and rewrite the Hamiltonian of

the doublet in the basis of circular polarizations in the form

$$H'_{\rm ax} = (\mathcal{A} + \mathcal{B})k^2 + \mathcal{B}[(k_x^2 - k_y^2)S_x + 2k_x k_y S_y]. \quad \text{(E5)}$$

[1] L. Lu, J. D. Joannopoulos, and M. Soljačić, Topological photonics, Nat. Photonics **8**, 821 (2014).

[2] T. Ozawa, H. M. Price, A. Amo, N. Goldman, M. Hafezi, L. Lu, M. C. Rechtsman, D. Schuster, J. Simon, O. Zilberberg, and I. Carusotto, Topological photonics, Rev. Mod. Phys. **91**, 015006 (2019).

[3] Y. Hatsugai, Chern Number and Edge States in the Integer Quantum Hall Effect, Phys. Rev. Lett. **71**, 3697 (1993).

[4] X.-L. Qi, Y.-S. Wu, and S.-C. Zhang, General theorem relating the bulk topological number to edge states in two-dimensional insulators, Phys. Rev. B **74**, 045125 (2006).

[5] S. Kawata, *Near-Field Optics and Surface Plasmon Polaritons* (Springer, Berlin, Heidelberg, 2001).

[6] A. V. Kavokin, I. A. Shelykh, and G. Malpuech, Lossless interface modes at the boundary between two periodic dielectric structures, Phys. Rev. B **72**, 233102 (2005).

[7] M. Kaliteevski, I. Iorsh, S. Brand, R. A. Abram, J. M. Chamberlain, A. V. Kavokin, and I. A. Shelykh, Tamm plasmon-polaritons: Possible electromagnetic states at the interface of a metal and a dielectric Bragg mirror, Phys. Rev. B **76**, 165415 (2007).

[8] I. Y. Chestnov, E. S. Sedov, S. V. Kutrovskaya, A. O. Kucherik, S. M. Arakelian, and A. V. Kavokin, One-dimensional Tamm plasmons: Spatial confinement, propagation, and polarization properties, Phys. Rev. B **96**, 245309 (2017).

[9] H. Y. Dong, J. Wang, and K. H. Fung, One-way optical tunneling induced by nonreciprocal dispersion of Tamm states in magnetophotonic crystals, Opt. Lett. **38**, 5232 (2013).

[10] A. Palatnik, M. Sudzius, S. Meister, and K. Leo, One-dimensional planar topological laser, Nanophotonics **10**, 2459 (2021).

[11] A. Askitopoulos, L. Mouchliadis, I. Iorsh, G. Christmann, J. J. Baumberg, M. A. Kaliteevski, Z. Hatzopoulos, and P. G. Savvidis, Bragg Polaritons: Strong Coupling and Amplification in an Unfolded Microcavity, Phys. Rev. Lett. **106**, 076401 (2011).

[12] E. S. Sedov, I. V. Iorsh, S. M. Arakelian, A. P. Alodjants, and A. Kavokin, Hyperbolic Metamaterials with Bragg Polaritons, Phys. Rev. Lett. **114**, 237402 (2015).

[13] E. S. Sedov, E. D. Cherotchenko, S. M. Arakelian, and A. V. Kavokin, Light propagation in tunable exciton-polariton one-dimensional photonic crystals, Phys. Rev. B **94**, 125309 (2016).

[14] F. Biancalana, L. Mouchliadis, C. Creatore, S. Osborne, and W. Langbein, Microcavity polaritonlike dispersion doublet in resonant Bragg gratings, Phys. Rev. B **80**, 121306 (2009).

[15] A. Kavokin, J. Baumberg, G. Malpuech, and F. Laussy, *Microcavities*, Series on Semiconductor Science and Technology. OUP Oxford, 2017), 2nd ed.

[16] G. Panzarini, L. C. Andreani, A. Armitage, D. Baxter, M. S. Skolnick, V. N. Astratov, J. S. Roberts, A. V. Kavokin, M. R. Vladimirova, and M. A. Kaliteevski, Exciton-light coupling in single and coupled semiconductor microcavities: Polariton dispersion and polarization splitting, Phys. Rev. B **59**, 5082 (1999).

[17] D. Schmidt, B. Berger, M. Bayer, C. Schneider, M. Kamp, S. Höfling, E. Sedov, A. Kavokin, and M. Aßmann, Dynamics of the optical spin hall effect, Phys. Rev. B **96**, 075309 (2017).

[18] H.-T. Lim, E. Togan, M. Kroner, J. Miguel-Sanchez, and A. Imamoğlu, Electrically tunable artificial gauge potential for polaritons, Nat. Commun. **8**, 14540 (2017).

[19] T. Godde, M. M. Glazov, I. A. Akimov, D. R. Yakovlev, H. Mariette, and M. Bayer, Magnetic field induced nutation of exciton-polariton polarization in (Cd, Zn)Te crystals, Phys. Rev. B **88**, 155203 (2013).

[20] O. V. Gogolin, V. A. Tsvetkov, and E. G. Tsitsishvili, Magnetically induced birefringence in cubic crystals, JETP **60**, 593 (1984).

[21] P. Yeh, Electromagnetic propagation in birefringent layered media, J. Opt. Soc. Am. **69**, 742 (1979).

[22] D. W. Berreman, Optics in stratified and anisotropic media: 4 × 4-matrix formulation, J. Opt. Soc. Am. **62**, 502 (1972).

[23] N. C. Passler and A. Paarmann, Generalized 4 × 4 matrix formalism for light propagation in anisotropic stratified media: Study of surface phonon polaritons in polar dielectric heterostructures, J. Opt. Soc. Am. B **34**, 2128 (2017).

[24] W. Xu, L. T. Wood, and T. D. Golding, Optical degeneracies in anisotropic layered media: Treatment of singularities in a 4 × 4 matrix formalism, Phys. Rev. B **61**, 1740 (2000).

[25] We take the following parameters of the layers of the structure. The dielectric constant of SiO_2 is $\varepsilon_a = 2.25$. The background dielectric constant of CdTe is $\varepsilon_{b0} = 7.8$, the LT splitting is $\hbar\omega_{\rm LT} = 0.14$ meV, the nonradiative decay rate is $\hbar\Gamma = 0.1$ meV, the Zeeman splitting constant is $\gamma_1 = 2 \times 10^{-4}$ T^{-1}, and the parameters of the magnetospatial dispersion are $g = -8 \times 10^{-4}$ μm T^{-1}, $h = 4 \times 10^{-3}$ μm T^{-1}. The thicknesses of the layers are $a^{\rm top} = 148.6$ nm, $b^{\rm top} = 164.1$ nm and $a^{\rm bot} = 101.8$ nm, $b^{\rm bot} = 54.5$ nm.

[26] L. V. Kotova, V. N. Kats, A. V. Platonov, V. P. Kochereshko, R. André, and L. E. Golub, Magnetospatial dispersion of semiconductor quantum wells, Phys. Rev. B **97**, 125302 (2018).

[27] The parameters in Hamiltonian (3) are as follows. The effective mass is $m^* = 3.2 \times 10^{-5} m_0$, where m_0 is the free electron mass, the Zeeman splitting constant is $C_1 = 15$ μeV T^{-1}, the TE-TM splitting constant is $C_2 = 0.5$ meVμm^2, and the magneto-induced dispersion constant is $C_3 = 30$ μeV μm T^{-1}.

[28] This situation is similar to the two-dimensional Dirac equation.

[29] A. Kavokin, G. Malpuech, and M. Glazov, Optical Spin Hall Effect, Phys. Rev. Lett. **95**, 136601 (2005).

[30] C. Leyder, M. Romanelli, J. P. Karr, E. Giacobino, T. C. H. Liew, M. M. Glazov, A. V. Kavokin, G. Malpuech, and A. Bramati, Observation of the optical spin hall effect, Nat. Phys. **3**, 628 (2007).

[31] D. Caputo, E. S. Sedov, D. Ballarini, M. M. Glazov, A. V. Kavokin, and D. Sanvitto, Magnetic control of polariton spin transport, Commun. Phys. **2**, 165 (2019).

[32] E. S. Sedov, Y. G. Rubo, and A. V. Kavokin, *Zitterbewegung* of exciton-polaritons, Phys. Rev. B **97**, 245312 (2018).

[33] E. S. Sedov, I. E. Sedova, S. M. Arakelian, and A. V. Kavokin, Magnetic control over the zitterbewegung of exciton–polaritons, New J. Phys. **22**, 083059 (2020).

[34] E. Sedov, I. Sedova, S. Arakelian, and A. Kavokin, Polygonal patterns of confined light, Opt. Lett. **46**, 1836 (2021).

[35] S. Klembt, T. H. Harder, O. A. Egorov, K. Winkler, R. Ge, M. A. Bandres, M. Emmerling, L. Worschech, T. C. H. Liew, M. Segev, C. Schneider, and S. Höfling, Exciton-polariton topological insulator, Nature **562**, 552 (2018).

[36] B. B. Krichevtsov, A. A. Rzhevskii, and H.-J. Weber, Second-order magnetoelectric susceptibility in the optical region of the boracite $Co_3B_7O_{13}I$, Phys. Rev. B **61**, 10084 (2000).

[37] B. B. Krichevtsov, R. V. Pisarev, A. A. Rzhevskii, V. N. Gridnev, and H. J. Weber, Magnetically induced spatial dispersion in the cubic magnetic semiconductors $Cd_{1-x}Mn_xTe$, J. Exp. Theor. Phys. **87**, 553 (1998).

[38] N. C. Passler and A. Paarmann, Generalized $4\times$ 4 matrix formalism for light propagation in anisotropic stratified media: Study of surface phonon polaritons in polar dielectric heterostructures: Erratum, J. Opt. Soc. Am. B **36**, 3246 (2019).

[39] N. C. Passler, M. Jeannin, and A. Paarmann, Layer-resolved absorption of light in arbitrarily anisotropic heterostructures, Phys. Rev. B **101**, 165425 (2020).